

# Learning to Navigate from Simulation via Spatial and Semantic Information Synthesis

Gang Chen, Hongzhe Yu, Wei Dong, Xinjun Sheng, Xiangyang Zhu and Han Ding

**Abstract**—While training an end-to-end navigation network in the real world is usually of high cost, simulations provide a safe and cheap environment in this training stage. However, training neural network models in simulations brings up the problem of how to effectively transfer the model from simulations to the real world (sim-to-real). We regard the environment representation as a crucial element in this transfer process. In this work, we propose a visual information pyramid (VIP) theory to systematically investigate a practical environment representation. A representation composed of spatial and semantic information synthesis is established based on this theory. Specifically, the spatial information is presented by a noise-model-assisted depth image while the semantic information is expressed with a categorized detection image. To explore the effectiveness of this representation, we first extract different representations from a same dataset collected from expert operations, then feed them to the same or very similar neural networks to train the network parameters, and finally evaluate the trained neural networks in simulated and real world navigation tasks. Results suggest that our proposed environment representation behaves best compared with representations popularly used in the literature. With mere one-hour-long training data collected from simulation, the network model trained with our representation can successfully navigate the robot in various scenarios with obstacles. Furthermore, an analysis on the feature map is implemented to investigate the effectiveness through inner reaction, which could be irradiative for future researches on end-to-end navigation.

**Index Terms**—Deep learning in robotics and automation, learning from demonstration, motion and path planning, simulation and animation

## I. INTRODUCTION

1) *Background*: The fundamental objective of mobile robot navigation is to arrive at a goal position without collision. The mobile robot is supposed to be aware of the obstacles and move freely in different working scenarios. Mathematically modeling various situations a mobile robot may encounter is hardly possible, while end-to-end learning provides a promising data-driven solution to this high-dimension problem. End-to-end learning maps sensor data directly to control outputs and has been proved to be promising in coping with many scenarios [1], [2], [3].

As a data-driven approach, end-to-end learning often requires a large amount of training data. While collecting

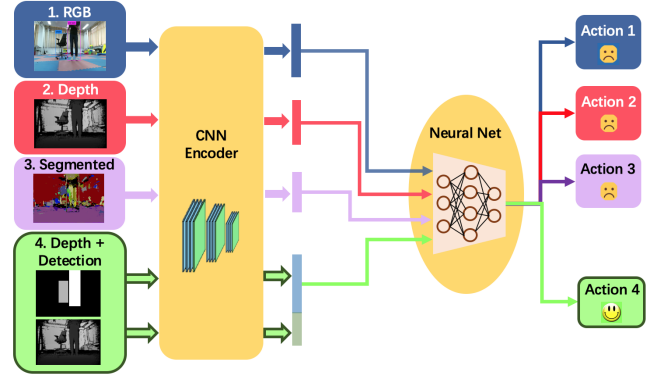


Fig. 1. Method Overview: Different environment representations are compared via the same neural network structure to evaluate their influence to the sim-to-real transfer process in indoor navigation tasks.

training data in the real world is usually of high cost, collecting data in simulation is much more convenient. Therefore, training the model in simulation and transfer it directly to the real world, namely sim-to-real learning, is an attractive approach. Many researches have studied sim-to-real learning for robot manipulators [4], [5]. The working environment of a robot manipulator is usually fixed and easy to model in simulation. However, the working environments of a mobile robot are often diversified. Subtly building these working environments in simulation is hardly possible. Under such circumstances, how to transfer the network model trained in a limited number of roughly simulated environments to various real-world scenarios has to be concerned.

To fulfill an effective transfer process, high generalization ability of the network is demanded. A crucial factor for this generalization ability is the environment representation [6]. As vision sensor provides abundant information of the view field, state-of-the-art works used RGB image [7], depth image [8] and segmented semantic image [9] as the representation in end-to-end navigation. However, no systematical theory is raised to compare these representations and explore a better representation.

2) *Our Approach*: Inspired by the visual information abstraction behavior of human operators, we propose the VIP theory for vision-based end-to-end navigation and derive three criteria for the paradigm of sim-to-real learning:

- semantic information
- spatial information
- noise model for the real world sensor

Accordingly, an environment representation composed of

\*This work is partially supported by the National Natural Science Foundation of China (Grant No. 51605282) and National Science and Technology Major Project (2017ZX01041101-003).

Gang Chen, Hongzhe Yu, Wei Dong, Xinjun Sheng, Xiangyang Zhu and Han Ding are with the State Key Laboratory of Mechanical System and Vibration, School of Mechanical Engineering, Shanghai Jiaotong University, Shanghai, 200240, China. (Corresponding author: Wei Dong. dr.dongwei@sjtu.edu.cn)

spatial and semantic information synthesis with modeled noise is designed. The spatial information is presented by a noise-model-assisted depth image while the semantic information is expressed with a categorized detection image. A dataset from expert operations in a simulated indoor scenario is obtained and networks models with our representation together with all the other representations which are to be compared are trained with this dataset. The performance of these models with different environment representations are evaluated in two approaches:

- Quantitatively, the trained models are tested both in another simulated scenario and in a real-world scenario.
- Intuitively, a fast comparison method is presented, which reveals the internal reactions of the network by constructing a feature map with the hidden convolutional layers of the network.

Both ways indicates our representation behaves best, which supports our VIP theory in turn.

3) *Contributions*: The contribution of this work is:

- Proposed the VIP theory and three criteria for the environment representation in vision-based sim-to-real navigation.
- Designed a representation with spatial and semantic information synthesis based on the theory, which also concerns the noise model in the real world.
- Presented a fast evaluation approach through constructing feature maps in CNN layers.

The related video of this work can be found at: <https://youtu.be/1lp417Y8Wb4>.

## II. RELATED WORK

### A. End-to-end learning

End-to-end learning dates back to the 1980s [10] and has been proved to be a promising approach in navigation tasks for mobile robots [11]. Benefiting from the development of deep neural networks in recent years, the performance of end-to-end learning based navigation has embraced a great improvement. The fundamental ability in navigation is obstacle avoidance. End-to-end learning networks have achieved compelling obstacle avoidance performance in many scenes, such as highway [12], trail [13] or corridor [2]. Global direction command given by a high level planner is also concerned in the literature [1], [14] to help robots make turns at intersections. A more complicated situation is in the environment with dynamic obstacles like pedestrians. The mobile robot must act more subtly and rapidly to avoid collision [15], [16].

### B. RGB image representation

In these learning-based navigation works, training data is important. However, operating a mobile robot to collect training data in the real world is inconvenient and time-consuming. Any damage to the environment or the robot itself could cause a lot of trouble. To enhance the efficiency in the data collection process, some researchers use the data acquired from the cameras mounted on a person [17], [13]

or a car [18] to imitate the behaviors of a mobile robot. Another effective approach is to use sim-to-real learning. Tai et al. [19] adopt few sparse distance points measured by laser range finders as the network input and achieve a good sim-to-real transferability in indoor environments without pedestrians. In vision-based navigation, several works use the RGB image as the environment representation for the sim-to-real learning networks. The RGB image can be directly fed to a single end-to-end network to get the control commands [20] or be divided into grids firstly to learn the best heading direction [7]. The result is excellent in simulation but less satisfying in the real-world tests. A special approach is to utilize two auto-encoders to generate a real RGB image from a simulated image [21]. This approach only suits a fixed number of simple scenarios since a refined mapping from simulated images to real images is quite difficult.

### C. Depth image representation

Except for the usage of RGB image, depth image has also been adopted in sim-to-real learning for mobile robots. Depth image is easy to acquire from a stereo camera or an RGB-D camera and has been proved to be an effective environment representation when training with the data collected in the real world [22], [3]. Few works have tried to train the network with simulated depth images. One recent work tries this the depth image based sim-to-real learning in a pedestrian-rich scenario [8]. The performance is excellent in simulation but barely satisfying in the real world due to the lack of modeling the noise in real depth images. The navigation model based on depth image trained for comparison in [23] behaves poorly out of the same reason.

### D. Semantic image representation

Motivated by the traditional free space searching and path planning paradigm, some works utilize a semantic image showing the free space area to form the environment representation. One implicit approach is to adopt an image segmentation network as semantic feature extraction layers and add new layers to output the control commands [24]. Another explicit approach with better performance is to generate a semantic segmentation image first and then feeds it to another network to get waypoints [9] or velocity output [23], [25]. However, this approach depends largely on the speed and accuracy of image segmentation in the real world. A better environment representation is still desired.

## III. METHODS

To systematically analyze the vision-based environment representation and explore a feasible representation for sim-to-real learning, a theory regarding visual navigation and three criteria are proposed in this section. Then a representation composed of spatial and semantic information synthesis is designed accordingly, in which the noise model is considered to further narrow the gap between simulation and the real world. Finally, the utilized training approach and network architecture is described.

### A. Design Criteria

Consider a human operator who controls a mobile robot remotely based on a camera view. The perception of the operator comes from an RGB image composed of basic intensity information on each pixel and textual information given by the distribution of the intensity. From these detailed low-level information the human operator can abstract high-level spatial and semantic information through his perception experience to the world and controls the robot based on these two kinds of high-level information. Thus when an new operating environment with different intensity or texture comes, the operator can still control the robot well. We define this process as a visual information pyramid (VIP), as is illustrated in Fig. 2.

Spatial information tells the layout of environment and the position of the obstacles. The importance of spatial information is intuitional and has also been proved in neural science area to have direct effect on entorhinal cortex, which is highly connected to people's navigation [?]. Meanwhile, semantic information distinguishes the objects to perform different behaviors. For instance, the operator would control the mobile robot to slow down to increase available reaction time and keep a relatively long distance when encountered with dynamic objects like pedestrians, while move fast and keep a shorter distance when encountered with a wall.

The low-level intensity information and textural information are the basis of spatial information and semantic information. Operator can only derive high-level information in the pyramid from low-level information. However, intensity information and textural information themselves matter little in navigation process. For example, the color of a obstacle would affect the navigation result much less than its distance and relative direction to the ego robot.

In vision-based sim-to-real learning, a basic principle is to make the input image in simulated training stage as similar as possible to the testing stage in the real world. Constructing sophisticated simulated environments to imitate the real working environments is difficult and expensive. Therefore, utilizing a rough simulated environment but a feasible environment representation that is able to keep the useful information while narrow the difference between simulation and the real world is a better solution. Intensity information and texture information differ a lot from simulation to the real world and from place to place while they matter little in navigation. On the contrary, high-level spatial information and semantic information differ little but are significant in navigation. Therefore, the first two criteria to design a environment representation for a high-performance sim-to-real navigation network are:

- The representation should express spatial information and semantic information as explicitly as possible.
- The representation should contain little dispensable information like intensity or texture information.

Observation results are usually perfect in simulation but noisy in the real world. To further narrow the gap between simulation and the real world, noise model of the environ-

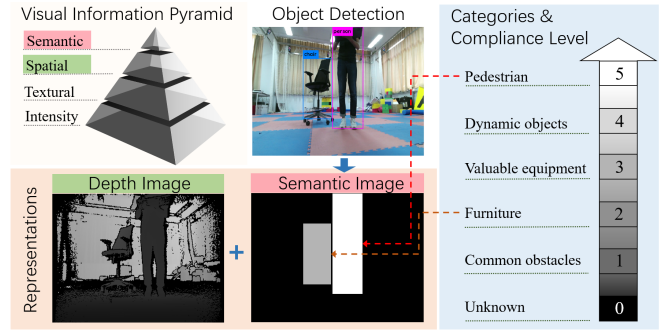


Fig. 2. The raised VIP theory for vision based navigation and our environment representation.

ment representation must be considered. Hence the third criterion is:

- The noise model of the representation should be easy to build.

### B. Environment Representation

RGB image, depth image and segmented semantic image are usually used in former end-to-end navigation works. In regard of sim-to-real learning approach, the representation of RGB image does not fit the first two criteria we proposed. It is difficult for an end-to-end navigation network to learn the high-level spatial and semantic information directly from RGB image and control commands pairs. The representation of depth image explicitly contains spatial information and can be quickly acquired by an RGB-D camera or a stereo camera, but the semantic information contained is obscure. The representation of segmented semantic image acquired from deep learning explicitly describes the semantic information but the spatial information is only coarsely given by the layout of segmented objects on the image.

In our environment representation, spatial information and semantic information are synthesized. Depth image considering real-world noise model is adopted to give the spatial information. Additionally, a semantic image made through the object detection results, such as the results from the Yolo V3 [26], is deployed to present the semantic information. Although object segmentation approaches could generate more elaborate semantic information containing free space area, they are not fast and stable enough to operate with on-board computers currently. Fast object detection results from Yolo V3 are sufficient to realize object-distinguishable obstacle avoidance. To further decrease the diversity and increase the generalization ability, the semantic labels of the detected objects are graded into six categories according to the collision risk level. The pedestrians have the highest level which means the robot should keep a far distance and stay slow when pedestrians show up. The final semantic image is a gray-scale image that has different intensities on the regions of different categories. The higher the risk level is, the larger intensity the region is filled. If two of the detected objects overlap on the image, the object with a higher risk level is shown. This semantic image is named as categorized

**Input:**  $I_{in}$  (original depth image),  $r$  (ratio of the masked depth values)

**Output:**  $I_{out}$  (the processed depth image with noise near the edge).

```

1:  $w \leftarrow I_{in}.width, h \leftarrow I_{in}.height, I_{out} \leftarrow I_{in}$ 
2: for  $step = 0$  to  $\frac{r \cdot w \cdot h}{2}$  do
3:    $(x_1, y_1) \leftarrow (Rand(x) \mid x \sim N(0, \frac{w}{\alpha}), |x| \leq \frac{w}{2}, Rand(y) \mid y \sim U(0, h))$ 
4:    $(x_2, y_2) \leftarrow (Rand(x) \mid x \sim U(0, w), Rand(y) \mid y \sim N(0, \frac{h}{\beta}), |y| \leq \frac{h}{2})$ 
5:   if  $x_1 < 0$  then
6:      $x_1 \leftarrow x_1 + w$ 
7:   end if
8:   if  $y_2 < 0$  then
9:      $y_2 \leftarrow y_2 + h$ 
10:  end if
11:   $I_{out}(x_1, y_1), I_{out}(x_2, y_2) \leftarrow 0$ 
12: end for

```

Fig. 3. The algorithm of adding a mask on the border of a depth image.

detection image to distinguish from the segmented semantic image.

Depth image is acquired in the real world is pretty noisy. One type of obvious noise lies on the edges of the objects in the view, which is usually subject to a Gaussian distribution. Our work uses the Kinect V2 RGB-D camera and the related noise model for the edges of objects has been studied in a previous work [27]. The mean of the noise is the true depth and the standard deviation can be described as:

$$\sigma(z) = (0.0012 + 0.0019(z - 0.4)^2) \cdot \xi \quad (1)$$

where  $z$  is the real depth and  $\xi \in [1.0, 1.2]$  is a random coefficient added to adjust extreme situations described in the previous work. Edges of objects are detected by the Canny algorithm [28].

Furthermore, we found that the depth near the border of the image is often unmeasurable. The situation varies a lot in different scenarios and different light conditions hence the noise is hard to accurately model. Considering the uncertainty of this noise, a mask following a combination of Gaussian distribution and uniform distribution is added to randomly remove some values on the border of the image. The algorithm is described in Fig. 3, where the input ratio of the masked depth values is sampled from 0% to 30%,  $\alpha$  is 36 and  $\beta$  is 24 for a depth image with  $640 \times 480$  pixels. Finally, the salt-and-pepper noise is added randomly on the whole image. A comparison between the original simulated depth image, the noised simulated image, and a real-world depth image is shown in Fig. 4.

In comparison, the networks that utilize depth image, RGB image and segmented semantic image without added noise as the environment representation are also tested in our experiments. The noise for RGB image follows the approach in [1], including the change in contrast, tone and brightness and the addition of Gaussian noise, Gaussian blur, and salt-and-pepper noise. The magnitude of every transformation for

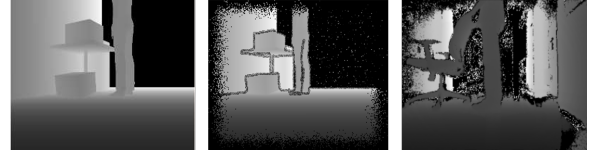


Fig. 4. A comparison of the simulated depth image, the simulated depth image with noise and the real world depth image (left to right).

each image is sampled randomly. As to the noise of segmented semantic image, we use the same segmentation deep learning model in the simulation to acquire the segmented semantic image rather than using the truth, thus the noise in simulation would be similar to the real world.

### C. Learning Approach

In order to prove the effectiveness of our environment representation, the training data for different representations should come from the same operation process of the robot. Hence we built a dataset from expert's first-person-view (FPV) operation in a simulated indoor environment in Gazebo [29] and utilized imitation learning paradigm to train the network models with different imported representations.

There are two assumptions in imitation learning. One is that the expert performs in the right way under all encountered situations. Another is that the learning network has the input which contains all the necessary information that leads the expert to his action. The first assumption can be satisfied by carefully operating the robot to acquire good moving paths. However, learning how to recover from mistakes is also quite important [30]. Therefore, we randomly initialized many bad situations, such as hitting an obstacle, as the start state to get recovering samples without importing the operations that brings the robot to these bad situations.

The second assumption is usually fulfilled by importing the same view that the expert had to the network. In our data collection stage, the view for the expert is an RGB image. According to our VIP theory, the expert infers the spatial information and the semantic information from the RGB image and operates mainly based on these two kinds of information. Our environment representation composed of a depth image and a categorized detection image contains these two kinds of necessary information and satisfies the assumption.

To accomplish a navigation task in an environment with intersections, which is very common in many working scenarios, a global direction command also needs to be considered. Following the similar way in [31], the direction commands consist of *move forward*, *turn left*, *turn right* and *stop*. The expert receives the direction command at each intersection from an arrow on the screen when collecting training data, while the network takes the direction command as an input in vector form. Denote the parameters in the network  $\theta$  and the expert action at a discrete time  $a_j$ , which includes linear velocity  $v$  and angular velocity  $\omega$ . Assume the network can be represented by a function  $F(e_j, c_j; \theta)$ , where  $e_j$  describes the input environment representation and



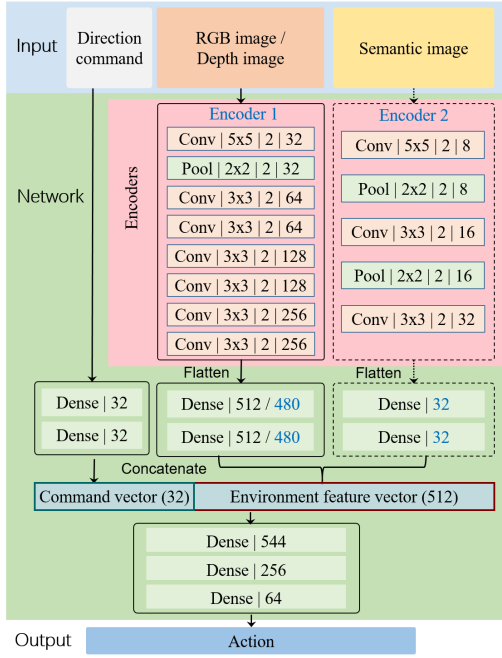


Fig. 5. The detailed structure of our network.

$c_j$  is the global direction command. The objective of our imitation learning can be expressed as:

$$\arg \min_{\theta} \sum_j \text{loss}(F(e_j, c_j; \theta), a_j) \quad (2)$$

#### D. Network Architecture

As has been proved in previous works on goal-directed imitation learning with image input [1],[31], utilizing convolutional layers to generate a vector from the input image and concatenating the vector with global direction commands is an effective network structure. The convolutional layers work as an encoder that extracts valuable features from the image. A similar modularized structure is adopted in our network. Detailed structure can be found in Fig. 5.

The input consists of environment representation and direction command. Four kinds of environment representations are considered for comparison, which are RGB image, depth image, segmented semantic image and our representation with both depth image and categorized detection image. In the first three cases, only Encoder 1 is used to extract the features from the RGB image, the depth image or the segmented semantic image. The result is flattened and imported to two dense layers with 512 neurons to get a feature vector. After that, the feature vector is concatenated with a command vector and then connected to another three dense layers to generate the final action. In the fourth case with both the depth image and the categorized detection image, two encoders are utilized. Encoder 1 stays the same except that the connected dense layers have 480 neurons each. Encoder 2 is added to extract features from the semantic image. The dense layers after Encoder 2 have only 32 neurons.

The depth image and the categorized detection image in the fourth case are processed with two encoders. As

a result, the information in the two images is not connected at the pixel-wise level. The final output can be treated as an overlay of the influence of the categorized detection image and the depth image. The pixel position and the depth value in the depth image give the network the spatial information of all objects in the view. Meanwhile, the intensity and pixel position in the categorized detection image give the network the semantic category of the detected objects as well as their imprecise spatial layouts. We tried to connect the depth image and the categorized detection image at the pixel-wise level via regarding them as two channels in one image. However, the result was terrible because our categorized detection image usually contains less valuable information than the depth image, especially when there is no object detected. Thus the semantic image is valued less with a separate network.

All the images have a size of  $256 \times 192$  pixels and the networks are light and fast to fit the real-time navigation tasks. The final output is an action vector containing linear and angular velocity control signals. Our loss function can be described as:

$$\text{loss}(a, a_{ref}) = \|v - v_{ref}\|^2 + \lambda \|\omega - \omega_{ref}\|^2 + \sum \gamma \theta_k^2 \quad (3)$$

The last component in this equation is the  $L2$  regularization item.  $\gamma$  is  $1 \times 10^{-7}$  for the weights in dense layers. The range of  $v$  and  $\omega$  is normalized before training.  $\lambda$  is a parameter to balance the effect of the error of linear and angular velocity. In practice,  $\lambda = 1$  works fine.

Moreover, a 50% dropout is applied after the convolutional layers and the first dense layer after concatenation. The ReLU nonlinearities are used for all hidden layers. The models were trained by Adam solver[32] with a mini-batch size of 40 and an initial learning rate of  $1 \times 10^{-4}$ .

#### E. Evaluation Approach

The commonly utilized evaluation approach for an end-to-end navigation network model is to conduct experiments in a testing environment and assess by indicators like collision-free moving time [14] or intervention times [1]. For the sim-to-real paradigm, models trained in simulation should be tested on the real-world robot system to get the evaluation result. However, in the early stage of research, testing the models directly in the real world can be dangerous and time-consuming. One way is to test the models in a simulated environment different from the training environment firstly to evaluate the generalization ability. The limitation is that the input observation is still simulated. Hence we propose a fast and intuitive approach to analyze the reaction of the network models with real observation. A typical real-world scenario is set up and the observed images are collected directly from the RGB-D camera on the robot. Then the images are imported to the network model trained in simulation and a feature map can be constructed with the middle convolutional layer of the network. The feature map intuitively reflects the reaction of the model towards different obstacles while it also reveals the effectiveness of different environment representations.

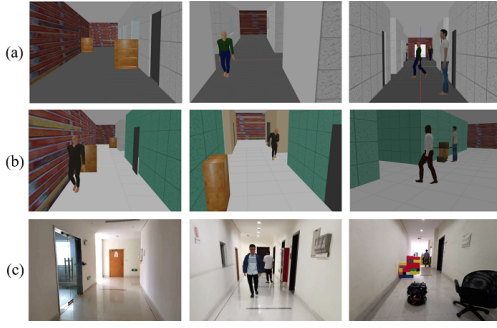


Fig. 6. The settings of the simulated training environment, the simulated testing environment and the real world testing environment (from Row (a) to Row (c)).



Fig. 7. The physical system to test the models.

The details can be found in the feature map analysis part in experiments section.

#### IV. EXPERIMENTS

We mainly focus on indoor scenarios in our experiments. All the training data came from a simple simulated environment built in Gazebo [29]. The results were firstly evaluated in a testing simulated environment and then in a real indoor environment to compare the results in both simulation and the real world. Experiments in several other real-world scenarios, including outdoor scenarios, were also conducted. The following presents our system and results.

##### A. System Setup

Two simulated indoor environments were built in Gazebo to train and test the models respectively. The mobile robot was a simulated TurtleBot. Compared to the training environment, the testing environment has a different building structure, and the appearances of some objects are also diverse. The settings of the simulated testing environment are shown in Fig. 6 and a map is presented in Fig. 8.

In the training process, the expert controlled the simulated mobile robot with a joystick in first-person view. No global route was planned and the expert followed a direction command generated randomly at each intersection. In the testing environment, the mobile followed a global route that could cover the whole map.

The physical system of the mobile robot is composed of a mobile platform, a bottom controller, an on-board computer and an RGB-D camera, as is shown in Fig. 7. Since planning global topology route is not our focus, a joystick is simply

utilized to send a direction command at each intersection. The on-board computer is mounted with an NVIDIA GTX 1060 GPU to run Yolo V3 and our end-to-end navigation models. The mobile robot moves at a speed of about 0.8 m/s, which is approximately the speed of walking.

To evaluate the models trained in simulation in the real world quantitatively, a place in our lab building was chosen as the real-world testing environment. The width of the corridors ranges from 2.0m to 3.2m. The mobile robot should pass corridors with a total length of about ninety meters. The start point and the end point shared the same place. We made the corridors cluttered with some chairs and foam boards. Some voluntary pedestrians confronted, crossed or overtook the mobile robot to test its ability to react to dynamical obstacles. The volunteers had no idea of which model was running during the tests. Fig. 9 shows a laser-scanned grid map of the real-world testing environment.

##### B. Evaluation

Three networks with RGB image, depth image, and both depth image and semantic image as environment representation were trained with and without augmented data. Hence six models were generated. Each model was trained 400 epochs with one-hour simulated training data. We evaluated the models in the testing environments and analyzed the reaction inside the networks later. Details are given below.

1) *Performance Evaluation*: The performance was firstly evaluated quantitatively through 12 trials for each model in the simulated testing environment and 5 trials in the real-world testing environment. The basic obstacle avoidance ability was evaluated by the average number of intervention times. An intervention happened when the robot hit an obstacle or was stuck in a certain situation.

It is crucial to quantify the ability to react to dynamical obstacles – in our case, the pedestrians. Previous works evaluated the ability by minimum distance to the pedestrians [33] or the successful times of avoiding hitting a pedestrian [16]. The limitation of these evaluating indicators is that they depend heavily on the compliance of pedestrians rather than the robot itself. Some pedestrians may intentionally or occasionally walk very close to the robot and cause a small minimum distance. Therefore, a more objective indicator free from the behaviors of pedestrians is necessary.

Intuitively, on the robot side, decelerating, waiting or turning to avoid colliding on the pedestrians show its reaction to the obstacles. In all these actions, the linear velocity of the robot would decrease. Thus the statistical average percentage of the linear velocity decrease, compared to the situation with no pedestrian nearby, was adopted to evaluate the ability to react to moving obstacles. The velocity decrease percentage was only calculated when there was a pedestrian in the view since the mobile robot could not respond to the pedestrian if the pedestrian was in the blind zone. The velocity was acquired by the ground truth in simulation and the motor encoders on the wheels in the real world. Furthermore, a score given by pedestrians after each real-world test was adopted to evaluate this ability subjectively.

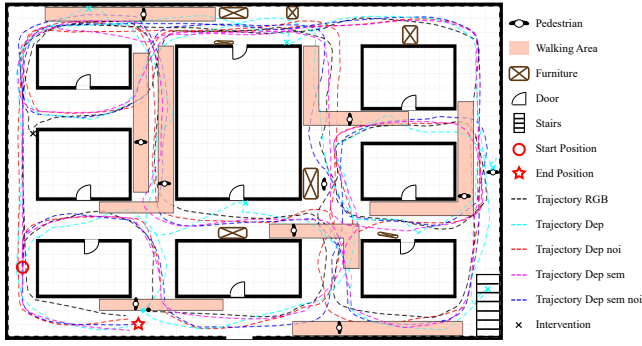


Fig. 8. A map of the simulated testing environment and typical trajectories of valid models.

TABLE I

RESULTS IN THE SIMULATED TESTING ENVIRONMENT.

Model	Interventions	Time (min)	Velocity decrease
RGB	2.50	7.27	41.5%
RGB noi.	-	-	-
Dep.	5.58	10.17	42.2%
Dep. noi.	0.58	<b>5.84</b>	32.4%
Dep. Sem.	0.92	6.21	<b>44.8%</b>
Dep. noi. Sem.	<b>0.18</b>	6.10	36.1%

All our models run at a frequency of over 20 Hz in both simulation and the real-world tests. Typical trajectories in the simulated testing environment and the quantitative results are shown in Fig. 8 and Tab. I respectively. The names of the models are given by keyword abbreviations of the corresponding training data. The model trained with non-noise depth images behaves terribly with many interventions, so does the model trained with non-noise RGB images. When the augmented noisy data is added, the RGB noi. model behaves worse and collides even over 30 times in a single trial. Quantitative result is unavailable thus the table is filled with dashes. Changes on the percentage of augmented data were tested but helped little. On the contrary, augmented noise in the depth images helps improve the performance on obstacle avoidance significantly. In our consideration, the augmentation for RGB images contains changes of contrast, tone, and brightness, which are designed to improve the generalization ability to the real world. However, the changes never happen in the testing simulated environment and bring negative effects. Meanwhile, depth images are much less diversified than RGB images, leading to a high possibility of overfitting. Augmented noise effectively prevents overfitting.

Compared to the models trained with only depth images, adding a semantic image improves the ability to avoid dynamical obstacles as expected. Moreover, the times of intervention reduces remarkably, because the semantic image raises stronger effects on the detected objects, such as furniture and pedestrians, and improves the obstacle avoidance ability. One defect is that the average time to finish one test increases slightly due to the velocity decrease. Considering the trade-off between the finishing time and the ability to safely navigate in the presence of moving obstacles, the Dep. noi. Sem. model behaves best in simulation tests.

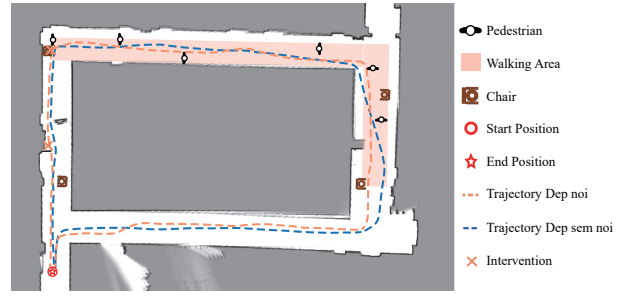


Fig. 9. A laser-scanned grid map of the real-world testing environment and trajectories of the two valid models.

TABLE II

RESULTS IN THE REAL-WORLD TESTING ENVIRONMENT.

Model	Interventions	Time (min)	Velocity decrease	Score (0-5)
Dep. noi.	3.00	<b>2.81</b>	7.2%	3.27
Dep. noi. Sem.	<b>0.80</b>	3.04	<b>12.2%</b>	<b>3.97</b>

In the real world testing environment, the mobile robot moved almost randomly when using the RGB model or the RGB noi. model, while staying still or keeping steering when using the non-noise depth or depth semantic model. Thus only the results of the rest two models are presented in Fig. 9 and Tab. II. In the ninety-meters-long real-world testing route with obstacles and pedestrians, our Dep. noi. Sem. model shows a striking result of less than one intervention in each trial averagely. The Dep. noi. model also works in the real world but the performance is less excellent. The relative performance of the two models keeps the same tendency in the simulation environment and the real-world environment.

In the evaluation of the ability of avoiding moving obstacles, the Dep. noi. Sem. model behaves much better both in the velocity decrease percentage and the subjective score given by pedestrians. An illustration of the velocity decrease percentage of the two models is given by Subplot (a) in Fig. 10. Compared to the values in simulations, the decrease percentage in the real world is less satisfying but acceptable because the behaviors of pedestrians in the real world are much more complicated. Subplot (b) presents two typical velocity command curves when the mobile robot confronts a pedestrian in the real world. The curves are aligned by

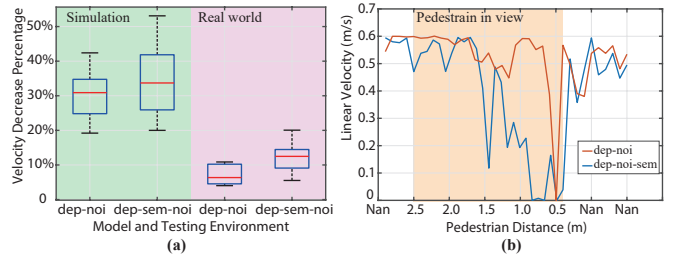


Fig. 10. A box plot of the velocity decrease percentage (Subplot (a)) and typical velocity command curves when the mobile robot confronts a pedestrian (Subplot (b)).



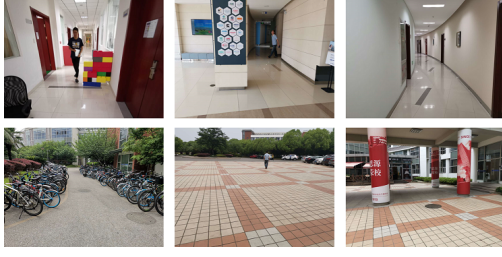


Fig. 11. Six testing environments for qualitative analysis.

the distance of the pedestrian to show the difference in the reaction distance. An obvious decrease in the output linear velocity command can be seen in both models when a pedestrian is close. The model imported with semantic image responses much earlier compared to the model without semantic image input.

The quantitative tests in the real world show that our Dep. noi. Sem. model, which has the environment representation composed of spatial and semantic information synthesis and considers noise model, performs the best in the real world. Besides, tests in a simulated environment different from the training environment could give a prior evaluation of the models before the real-world tests. We further test our best model qualitatively in six testing environments, which are shown in Fig. 11. Three of the environments are indoor and the rest are outdoor. Our model never met similar environments in the simulated training environment, but it is still able to avoid the obstacles and show social compliance. Due to the influence of sunlight, the depth image outdoors is pretty noisy while our model also performs well.

**2) Feature Map Analysis:** To study the internal effect of the environment representations, we set up a scenario with a pedestrian and two walls with different appearances and analyzed the feature maps for different environment representations in this scenario. The utilized network models are trained with augmented data and the results are presented in Fig. 12. Column (a) gives a composite view of the three kinds of environment representations. The pixels where the depth can be measured are painted in their real RGB color and the rest are painted in black. The person is detected and shown with a pink rectangle. Column (b) to (d) illustrate the states of the middle convolutional layer in the encoders for RGB image, depth image, and semantic image respectively. The middle layer is chosen because it extracts the useful features for navigation and is not too abstract to understand. The sum of the output matrix of each channel is normalized to generate the feature map. In the row order, the pedestrian showed up and came closer and closer to the mobile robot. The bars on the top of the images show the mean-squared error (MSE) of the corresponding image compared to the situation without any pedestrian. Larger MSE indicates a higher response towards the pedestrian.

The encoder network trained with RGB image has no obvious reaction to the pedestrian, no matter how close the pedestrian is. In the meantime, the white wall on the right is clearly shown in the feature map while the colorful wall on

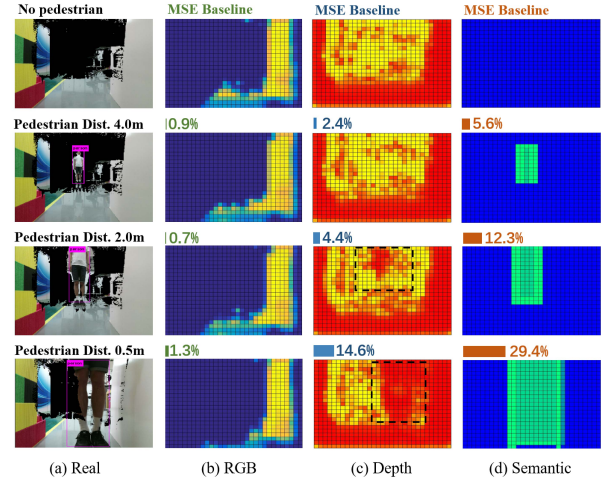


Fig. 12. The feature maps of the middle hidden layer in the encoders for different kinds of environment representations.

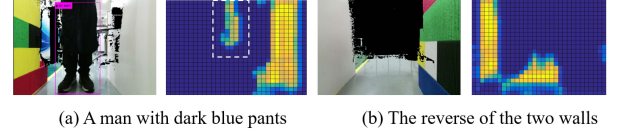


Fig. 13. The feature maps of the middle hidden layer in the RGB image encoder in two situations.

the left is not. The reason is that in the simulated training environment, the walls are mostly white and the people wear dark blue pants. Fig. 13 presents two more situations for the RGB image trained model. When the pedestrian wears a dark blue pant like the people in the simulation, some features clearly occur. When the position of the two walls is reversed, the area where the colorful wall is still has no features. Meanwhile, the features corresponding to the ground change because the brightness is higher due to the reflection of the white wall. This shows that the model trained with RGB image and control command pairs works mainly at the intensity level. Spatial or semantic information is hardly learned. Objects in the real world environment with different appearance raise little response.

The feature map of the depth image encoder (Column (c) in Fig. 12) shows better results. The effect of the walls on both sides can be seen clearly. The response to the pedestrian becomes obvious when the distance is shorter than 2.0 meters (reflected by the area in the dashed box and the MSE).

The semantic image is relatively simple but has the strongest response to the pedestrian. The corresponding feature map shows a rectangle representing the person, which is similar to the input semantic image. The main difference is that the intensity of the edge is higher than the inside. This is reasonable because the edge indicates the geometric layout of the pedestrian in the image, which matters in collision avoidance and social compliance. Compared to RGB image, depth image and the semantic image arouse much more obvious reactions in the real world.



## V. CONCLUSION

This work demonstrates the significance of environment representation in sim-to-real transfer learning for visual navigation. Bridging the gap between simulation and the real world requires high-level spatial and semantic connection from environment representation to control commands. Our representation composed of a depth image and a semantic image explicitly presents the spatial and semantic information in the view and successfully establishes this connection. Particularly, the depth image can realize obstacle avoidance in the real world when the noise model is considered. The semantic image enables a pedestrian-aware navigation and enhances both obstacle avoidance and social compliance capability. Further analysis on feature maps also proves the effectiveness of this environment representation.

Encouraging as the results are, a lot of effort remains before practical deployment. One limitation of this work is that the control commands are generated based only on the camera view at one frame while navigation is a continuous process related to former perceptions. Future works will consider the fusion of these perceptions in the network to realize better performance.

## REFERENCES

- [1] F. Codevilla, M. Müller, A. López, V. Koltun, and A. Dosovitskiy, "End-to-end driving via conditional imitation learning," in *IEEE International Conference on Robotics and Automation (ICRA)*, 2018, pp. 1–9.
- [2] D. Gandhi, L. Pinto, and A. Gupta, "Learning to fly by crashing," in *IEEE/RSJ International Conference on Intelligent Robots and Systems (IROS)*, 2017, pp. 3948–3955.
- [3] S. Hornauer, K. Zipser, and S. Yu, "Imitation learning of path-planned driving using disparity-depth images," in *European Conference on Computer Vision (ECCV)*. Springer, 2018, pp. 542–548.
- [4] A. A. Rusu, M. Večerík, T. Rothörl, N. Heess, R. Pascanu, and R. Hadsell, "Sim-to-real robot learning from pixels with progressive nets," in *Conference on Robot Learning (CoRL)*, 2017, pp. 262–270.
- [5] U. Viereck, A. t. Pas, K. Saenko, and R. Platt, "Learning a visuomotor controller for real world robotic grasping using simulated depth images," in *Conference on Robot Learning (CoRL)*, 2017, pp. 291–300.
- [6] L. Frommberger, "Generalization and transfer learning in noise-affected robot navigation tasks," in *Portuguese Conference on Artificial Intelligence*. Springer, 2007, pp. 508–519.
- [7] F. Sadeghi and S. Levine, "Cad2rl: Real single-image flight without a single real image," *Robotics: Science and Systems (RSS)*, 2017.
- [8] L. Tail, J. Zhang, M. Liu, and W. Burgard, "Socially compliant navigation through raw depth inputs with generative adversarial imitation learning," in *IEEE International Conference on Robotics and Automation (ICRA)*, 2018, pp. 1111–1117.
- [9] M. Mueller, A. Dosovitskiy, B. Ghanem, and V. Koltun, "Driving policy transfer via modularity and abstraction," in *Conference on Robot Learning (CoRL)*, 2018, pp. 1–15.
- [10] D. A. Pomerleau, "Alvin: An autonomous land vehicle in a neural network," in *Advances in neural information processing systems*, 1989, pp. 305–313.
- [11] U. Muller, J. Ben, E. Cosatto, B. Flepp, and Y. L. Cun, "Off-road obstacle avoidance through end-to-end learning," in *Advances in neural information processing systems*, 2005, pp. 739–746.
- [12] C. Chen, A. Seff, A. Kornhauser, and J. Xiao, "Deepdriving: Learning affordance for direct perception in autonomous driving," in *IEEE International Conference on Computer Vision (ICCV)*, 2015, pp. 2722–2730.
- [13] N. Smolyanskiy, A. Kamenev, J. Smith, and S. Birchfield, "Toward low-flying autonomous mav trail navigation using deep neural networks for environmental awareness," in *IEEE/RSJ International Conference on Intelligent Robots and Systems (IROS)*, 2017, pp. 4241–4247.
- [14] W. Gao, D. Hsu, W. S. Lee, S. Shen, and K. Subramanian, "Intention-net: Integrating planning and deep learning for goal-directed autonomous navigation," in *Conference on Robot Learning (CoRL)*, 2017, pp. 185–194.
- [15] N. Patel, A. Choromanska, P. Krishnamurthy, and F. Khorrami, "Sensor modality fusion with cnns for ugv autonomous driving in indoor environments," in *IEEE/RSJ International Conference on Intelligent Robots and Systems (IROS)*, 2017, pp. 1531–1536.
- [16] J. Bi, T. Xiao, Q. Sun, and C. Xu, "Navigation by imitation in a pedestrian-rich environment," *arXiv preprint arXiv:1811.00506*, 2018.
- [17] A. Giusti, J. Guzzi, D. C. Cireşan, F.-L. He, J. P. Rodríguez, F. Fontana, M. Faessler, C. Forster, J. Schmidhuber, G. Di Caro, *et al.*, "A machine learning approach to visual perception of forest trails for mobile robots," *IEEE Robotics and Automation Letters*, vol. 1, no. 2, pp. 661–667, 2015.
- [18] A. Loquercio, A. I. Maqueda, C. R. Del-Blanco, and D. Scaramuzza, "Dronet: Learning to fly by driving," *IEEE Robotics and Automation Letters*, vol. 3, no. 2, pp. 1088–1095, 2018.
- [19] L. Tai, G. Paolo, and M. Liu, "Virtual-to-real deep reinforcement learning: Continuous control of mobile robots for mapless navigation," in *IEEE/RSJ International Conference on Intelligent Robots and Systems (IROS)*, 2017, pp. 31–36.
- [20] H. Bharadhwaj, Z. Wang, Y. Bengio, and L. Paull, "A data-efficient framework for training and sim-to-real transfer of navigation policies," *arXiv preprint arXiv:1810.04871*, 2018.
- [21] X. Pan, Y. You, Z. Wang, and C. Lu, "Virtual to real reinforcement learning for autonomous driving," *arXiv preprint arXiv:1704.03952*, 2017.
- [22] L. Tai, S. Li, and M. Liu, "A deep-network solution towards model-less obstacle avoidance," in *IEEE/RSJ international conference on intelligent robots and systems (IROS)*, 2016, pp. 2759–2764.
- [23] Z.-W. Hong, C. Yu-Ming, S.-Y. Su, T.-Y. Shann, Y.-H. Chang, H.-K. Yang, B. H.-L. Ho, C.-C. Tu, Y.-C. Chang, T.-C. Hsiao, *et al.*, "Virtual-to-real: Learning to control in visual semantic segmentation," *arXiv preprint arXiv:1802.00285*, 2018.
- [24] H. Xu, Y. Gao, F. Yu, and T. Darrell, "End-to-end learning of driving models from large-scale video datasets," in *IEEE Conference on Computer Vision and Pattern Recognition (CVPR)*, 2017, pp. 3530–3538.
- [25] A. Mousavian, A. Toshev, M. Fiser, J. Kosecka, A. Wahid, and J. Davidson, "Visual representations for semantic target driven navigation," *arXiv preprint arXiv:1805.06066*, 2018.
- [26] J. Redmon and A. Farhadi, "Yolov3: An incremental improvement," *arXiv preprint arXiv:1804.02767*, 2018.
- [27] C. V. Nguyen, S. Izadi, and D. Lovell, "Modeling kinect sensor noise for improved 3d reconstruction and tracking," in *International Conference on 3D Imaging, Modeling, Processing, Visualization and Transmission (3DIMPVT)*, 2012, pp. 524–530.
- [28] J. Canny, "A computational approach to edge detection," in *Readings in computer vision*. Elsevier, 1987, pp. 184–203.
- [29] N. Koenig and A. Howard, "Design and use paradigms for gazebo, an open-source multi-robot simulator," in *IEEE/RSJ International Conference on Intelligent Robots and Systems (IROS)*, vol. 3, 2004, pp. 2149–2154.
- [30] S. Ross, G. J. Gordon, and J. A. Bagnell, "No-regret reductions for imitation learning and structured prediction," in *International Conference on Artificial Intelligence and Statistics (AISTATS)*, 2011.
- [31] A. Sauer, N. Savinov, and A. Geiger, "Conditional affordance learning for driving in urban environments," in *Conference on Robot Learning (CoRL)*, 2018, pp. 237–252.
- [32] D. Kingma and J. Ba, "Adam: A method for stochastic optimization," *International Conference on Learning Representations (ICLR)*, 2015.
- [33] Y. F. Chen, M. Everett, M. Liu, and J. P. How, "Socially aware motion planning with deep reinforcement learning," in *IEEE/RSJ International Conference on Intelligent Robots and Systems (IROS)*, 2017, pp. 1343–1350.